Turkish Journal of Electrical Engineering & Computer Sciences

http://journals.tubitak.gov.tr/elektrik/

Research Article

Turk J Elec Eng & Comp Sci
(2017) 25: 3591 – 3606
© TÜBİTAK
doi:10.3906/elk-1601-230

Performance comparison of the notable acceleration- and angle-based guidance laws for a short-range air-to-surface missile

Bülent ÖZKAN[1,*], **Mustafa Kemal ÖZGÖREN**[2], **Gökmen MAHMUTYAZICIOĞLU**[3]
[1]Defense Industries Research and Development Institute (TÜBİTAK SAGE),
Scientific and Technological Research Council of Turkey, Defense Industries Research and Development Institute, Ankara, Turkey
[2]Department of Mechanical Engineering, Middle East Technical University, Ankara, Turkey
[3]ROKETSAN A.Ş., Ankara, Turkey

Received: 20.01.2016 • **Accepted/Published Online:** 10.02.2017 • **Final Version:** 05.10.2017

Abstract: Short-range air-to-surface missiles have become globally popular in the last two decades. As a performance driver, the type of guidance law gains importance. In this study, proportional navigation, velocity pursuit, and augmented proportional navigation guidance laws, whose resulting guidance commands take the form of lateral acceleration, are applied to a short-range air-to-surface missile against both stationary and maneuvering ground targets. Body pursuit and linear homing guidance laws, which yield angular commands, are additionally applied. Having completed the relevant computer simulations, we conclude that none of the acceleration- and angle-based guidance laws are absolutely superior to the others.

Key words: Guidance, control, short-range missile, air-to-surface missile

1. Introduction

In recent years, the attack concept has evolved from mass destruction to point-hitting. In this context, guided munitions, including homing missiles and guided bombs, have gained more significance. When the range to the aimed target point becomes large, homing missiles are preferred to guided bombs. Here, the selection of a proper guidance law comes into the picture depending on the target type and certain operational requirements such as final miss distance goal, maximum acceleration demand, and total energy consumption [1–3]. Derived from the engagement geometry between the munition and target, guidance laws can be categorized in different manners. Among them, one classification is based on the type of guidance commands [1,4–6]. Namely, the guidance laws whose commands are generated in the form of lateral acceleration components of the munition can be called "acceleration-based guidance laws", while those whose commands are in the form of selected orientation angles are termed as "angle-based guidance laws" [4,7].

In this study, the performance comparison of notable acceleration- and angle-based guidance laws is investigated. As the proportional navigation guidance (PNG), velocity pursuit guidance (VPG), and augmented proportional navigation guidance (APNG) laws are handled in the former class, the body pursuit guidance (BPG) and linear homing guidance (LHG) laws are evaluated within the second category of guidance laws. The results of the computer simulations conducted in MATLAB Simulink are submitted for the guidance and control scheme constructed. The most significant contribution of this work to the literature is its evaluation of the widely

*Correspondence: bulent.ozkan@tubitak.gov.tr

used acceleration- and angle-based guidance laws on a suitably selected missile model in a comparative manner and in accordance with quantitative results.

2. Missile dynamic model

The governing equations of motion of the air-to-surface missile under consideration are shown in Figure 1, where C_M and δ_i denote the mass center of the missile. Deflection of control fin i for i = 1, 2, 3, and 4 can be determined using the Newton–Euler approach in the body-fixed frame of the missile (F_b), as given below [4,8]:

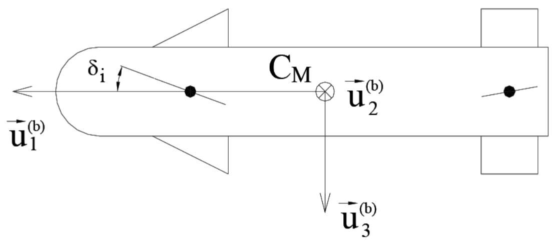

Figure 1. The considered missile model.

$$\dot{u} - r\,v + q\,w = (X + X_T)\,/m + g_x \tag{1}$$

$$\dot{v} + r\,u - p\,w = (Y + Y_T)\,/m + g_y \tag{2}$$

$$\dot{w} - q\,u + p\,v = (Z + Z_T)\,/m + g_z \tag{3}$$

$$\dot{p} = (L + L_T)\,/I_a \tag{4}$$

$$\dot{q} - p\,r = (M + M_T)\,/I_t \tag{5}$$

$$\dot{r} + p\,q = (N + N_T)\,/I_t \tag{6}$$

As m, I_a, and I_t stand for the mass, axial, and lateral moment of the inertia components of the missile, the parameters in Eqs. (1)–(6) are defined in the directions of the unit vectors of F_b, i.e. $\vec{u}_1^{(b)}$, $\vec{u}_2^{(b)}$, and $\vec{u}_3^{(b)}$, in the following manner:

p, q, and r: Roll, pitch, and yaw components of the missile angular velocity

u, v, and w: Linear velocity components of the missile

X, Y, and Z: Aerodynamic force components acting on the missile mass center

L, M, and N: Roll, pitch, and yaw components of the aerodynamic moment

X_T, Y_T, and Z_T: Thrust force components on the missile at its mass center

L_T, M_T, and N_T: Thrust misalignment moment components on the missile

g_x, g_y, and g_z: Gravity components acting on the missile at its mass center

When Eqs. (4)–(6) are examined, it is seen that the cross-products of the moment of inertia components are not considered; instead, only moment of inertia terms on the main diagonal of the inertia matrix are taken into account. This is because the considered missile model schematized in Figure 1 has rotational symmetries in both orthogonal lateral planes.

Eqs. (1)–(6) can be simplified for the after-boost guidance phase as

$$\dot{u} - r\,v + q\,w = (X/m) + g_x \tag{7}$$

$$\dot{v} + r\,u - p\,w = (Y/m) + g_y \tag{8}$$

$$\dot{w} - q\,u + p\,v = (Z/m) + g_z \tag{9}$$

$$\dot{p} = L/I_a \tag{10}$$

$$\dot{q} - p\,r = M/I_t \tag{11}$$

$$\dot{r} + p\,q = N/I_t \tag{12}$$

3. Missile aerodynamic model

Aerodynamic force and moment terms in Eqs. (7)–(12) can be approximated in terms of dynamic pressure (q_∞), missile cross-sectional area (S_M), and missile diameter (d_M), as follows [4,9]:

$$X = C_x\, q_\infty\, S_M \tag{13}$$

$$Y = C_y\, q_\infty\, S_M \tag{14}$$

$$Z = C_z\, q_\infty\, S_M \tag{15}$$

$$L = C_l\, q_\infty\, S_M\, d_M \tag{16}$$

$$M = C_m\, q_\infty\, S_M\, d_M \tag{17}$$

$$N = C_n\, q_\infty\, S_M\, d_M \tag{18}$$

Here q_∞ and S_M can be determined using air density (ρ) at the related altitude. v_M stands for the magnitude of the missile velocity for $\pi \approx 3.14$, as in [10]

$$q_\infty = (1/2)\ \rho\, v_M^2 \tag{19}$$

$$S_M = (\pi/4)\ d_M^2 \tag{20}$$

Aerodynamic coefficients C_x, C_y, C_z, C_l, C_m, and C_n can be expressed as the functions of angle of attack (α), side-slip angle (β), aileron, elevator, rudder deflections (δ_a, δ_e, and δ_r), p, q, and r in the following manner [4]:

$$C_x = C_{x0} \tag{21}$$

$$C_y = C_{y_\beta}\, \beta + C_{y_\delta}\, \delta_r + C_{y_r} \tau\, r \tag{22}$$

$$C_z = C_{z_\alpha}\,\alpha + C_{z_\delta}\,\delta_e + C_{z_q}\,\tau\,q \tag{23}$$

$$C_l = C_{l_\delta}\,\delta_a + C_{l_p}\,\tau\,p \tag{24}$$

$$C_m = C_{m_\alpha}\,\alpha + C_{m_\delta}\,\delta_e + C_{m_q}\,\tau\,q \tag{25}$$

$$C_n = C_{n_\beta}\,\beta + C_{n_\delta}\,\delta_r + C_{n_r}\,\tau\,r, \tag{26}$$

where $\tau = d_M/(2\,v_M)$ and C_{x0} is the static axial aerodynamic force component.

Stability derivatives C_{y_β}, C_{y_δ}, C_{y_r}, C_{z_α}, C_{z_δ}, C_{z_q}, C_{l_δ}, C_{l_p}, C_{m_α}, C_{m_δ}, C_{m_q}, C_{n_β}, C_{n_δ}, and C_{n_r} are dependent on the Mach number (M_∞) and are updated during the flight in the simulations. Here α and β can be defined as in Figure 2 [10]:

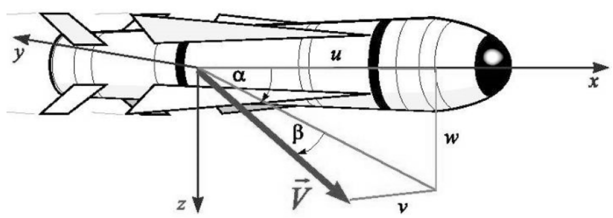

Figure 2. Demonstration of angle of attack and side-slip angle [10].

$$\alpha = \arctan\left(w/u\right) \tag{27}$$

$$\beta = \arcsin\left(v/v_M\right) \tag{28}$$

Deflection angles δ_a, δ_e, and δ_r are introduced in terms of the fin deflections with respect to the fin arrangement given in Figure 3, as follows [4]:

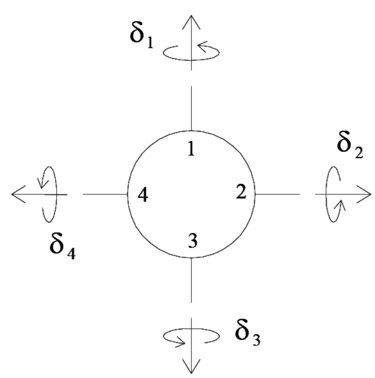

Figure 3. Considered fin arrangement from the rear view of the missile.

$$\delta_a = \left(\delta_1 + \delta_3\right)/2 \tag{29}$$

$$\delta_e = \left(\delta_2 - \delta_4\right)/2 \tag{30}$$

$$\delta_r = \left(\delta_1 - \delta_3\right)/2 \tag{31}$$

4. Guidance laws

The guidance laws that are utilized to steer the missile towards the predefined target are dealt with according to the type of guidance command. Namely, the guidance laws yielding commands in the form of lateral acceleration components of the missile and relevant orientation angles are chosen as the acceleration- and angle-based guidance laws, respectively.

4.1. Acceleration-based guidance laws

4.1.1. Proportional navigation guidance law

For the engagement geometry in Figure 4, where $\vec{u}_1^{(w)}$ and $\vec{u}_1^{(r)}$ stand for the first unit vectors of the wind frame (F_w) and line-of-sight (LOS) frame (F_r) along the missile velocity vector $(\vec{v}_{M/O_e})$ and LOS vector $(\vec{r}_{T/M})$, the command accelerations, i.e. a_{w2}^c and a_{w3}^c, drawn in Figures 5 and 6, can be found as in [4,6,9,11–13]:

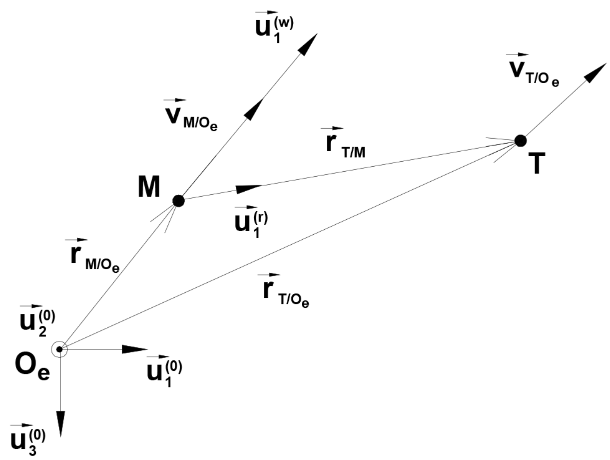

Fgure 4. Engagement geometry between the missile and target.

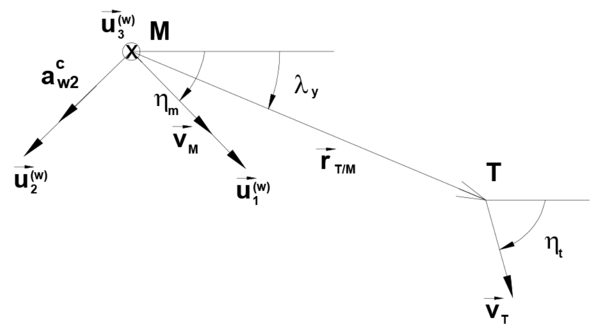

Figure 5. Horizontal plane of the wind frame.

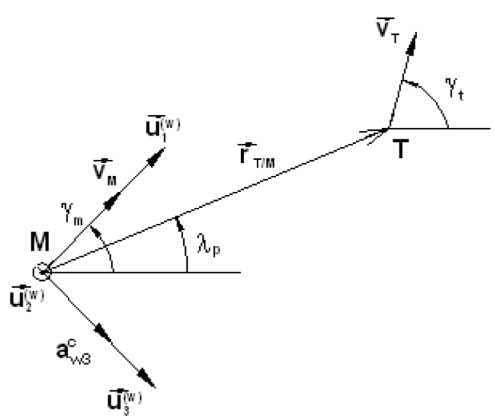

Figure 6. Vertical plane of the wind frame.

$$a_{w2}^c = N_2\, v_M\, \left[\dot{\lambda}_y\, \cos(\gamma_m) - \dot{\lambda}_p\, \sin(\gamma_m)\, \sin(\lambda_y - \eta_m)\right] \tag{32}$$

$$a_{w3}^c = -N_3\, v_M\, \dot{\lambda}_p\, \cos(\lambda_y - \eta_m) \tag{33}$$

Here N_2 and N_3 denote the effective navigation ratios in the pitch and yaw planes, λ_y and λ_p are the yaw and pitch angles of the LOS vector, η_m and γ_m indicate the flight path angles of the missile in the yaw and pitch planes, and $a^c_{w2} = a_{yd}$ and $a^c_{w3} = a_{zd}$ represent the desired values of the missile lateral accelerations.

4.1.2. Velocity pursuit guidance law

The VPG law, which dictates the alignment of $\vec{v}_{M/O_e}$ with $\vec{r}_{T/M}$, can be derived from the PNG law by treating N_2 and N_3 as unified in Eqs. (32) and (33) [7].

4.1.3. Augmented proportional navigation guidance law

Accounting the product of half of the relevant lateral acceleration component of the target by the corresponding effective navigation ratio in Eqs. (32) and (33), the acceleration commands can be found according to the APNG law as shown below [1,4,6]:

$$\begin{aligned} a^c_{w2} \;\; = \;\; & N_2 \Big\{ v_M \left[\dot{\lambda}_y \cos(\gamma_m) - \dot{\lambda}_p \sin(\gamma_m) \sin(\lambda_y - \eta_m) \right] \\ & + \left[a^n_T \cos(\eta_m - \eta_t) - a^t_T \sin(\eta_m - \eta_t) \right] / 2 \} \end{aligned} \tag{34}$$

$$a^c_{w3} = -N_3 \left\{ v_M \, \dot{\lambda}_p \cos(\lambda_y - \eta_m) + \left[a^t_T \cos(\eta_m - \eta_t) + a^n_T \sin(\eta_m - \eta_t) \right] \sin(\gamma_m)/2 \right\}, \tag{35}$$

where a^n_T and a^t_T are the normal and tangential components of the target acceleration vector, and η_t shows the heading angle of the target.

4.2. Angle-based guidance laws

4.2.1. Body pursuit guidance law

BPG law must coincide the longitudinal axis of the missile, i.e. $\vec{u}^{(b)}_1$ axis, with the LOS. Therefore, the guidance commands in the pitch and yaw planes (θ^c and ψ^c) can be derived, as θ and ψ denote the pitch and yaw angles of the missile [1,4]:

$$\theta^c = \lambda_p \tag{36}$$

$$\psi^c = \lambda_y \tag{37}$$

4.2.2. Linear homing guidance law

LHG law aims to maintain the missile on the collision triangle shaped by the missile, target, and predicted intercept point, as depicted in Figure 7. In Figure 7, M, T, and P stand for the missile, target, and predicted intercept point, respectively. $\vec{v}_{Mactual}$ and $\vec{v}_{Mideal}$ demonstrate the velocity vector of the missile at the beginning of the guidance and desired velocity vector, by orienting the missile velocity vector towards the predicted intercept point, where the collision of the missile with the target will occur afterwards [4].

As Δt indicates the time interval between initial time (t_0) and end of the intercept (t_F), the desired position vectors of the missile and target at point P can be written as

$$\vec{r}_j(t_F) = \vec{r}_j(t_0) + \vec{v}_{j/O_e} \Delta t, \tag{38}$$

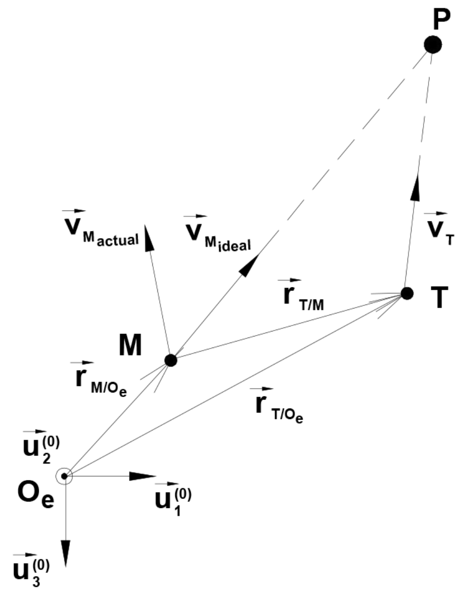

Figure 7. Linear homing guidance law geometry.

where for j = M and T, $\vec{r}_j = \vec{r}_{j/O_e}$.

Using Eq. (38), the guidance command to the flight path angle of the missile in the yaw plane (η_m^c) is obtained as follows, provided that $\cos(\gamma_m) \neq 0$ [4,14]:

$$\eta_m^c = \arctan\left[(v_{Ty}\,\Delta t - \Delta y)\,/\,(v_{Tx}\,\Delta t - \Delta x)\right] \tag{39}$$

Similarly, the guidance command in the pitch plane (γ_m^c) can be derived as in [4,14]:

$$\gamma_m^c = \arctan\left[\frac{\Delta z - v_{Tz}\,\Delta t}{(v_{Tx}\,\Delta t - \Delta x)\,\cos(\eta_m) + (v_{Ty}\,\Delta t - \Delta y)\,\sin(\eta_m)}\right] \tag{40}$$

Here Δx, Δy, and Δz are the components of the relative position vector between the missile and target, and v_{Tx}, v_{Ty}, and v_{Tz} are the velocity components of the target.

5. Missile control system

Two different missile control systems, i.e. missile autopilots, are modeled for the pitch and yaw planes of the missile, in order to convert the commands yielded by the considered guidance laws. It is assumed that the roll motion of the missile is compensated by means of a faster roll autopilot at the beginning of the motion. Here the pitch and yaw dynamics of the missile are decoupled by prior roll compensation. In order to maintain the stability of both types of control systems, an adaptive control strategy is constructed, which updates the relevant controller gains by changing the aerodynamic coefficients instantaneously in accordance with the present values of M_∞, α or β, and altitude.

5.1. Acceleration control system

The acceleration control systems are designed to realize the guidance commands generated by the PNG, VPG, and APNG laws for both the pitch and yaw planes.

The closed loop transfer function between the desired and actual lateral accelerations in the pitch plane (a_{zd} and a_z) can be written with regard to the block diagram of the control system, based on the classical proportional plus integral (PI) control action with the pitch damping term, as given in Figure 8 [4,15]:

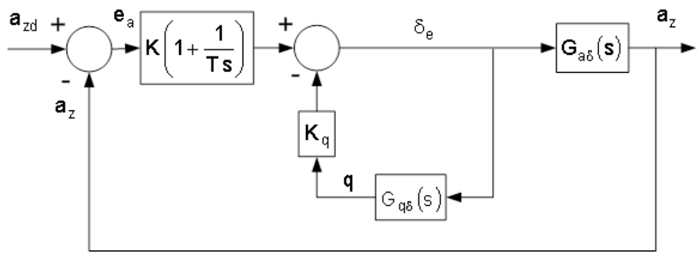

Figure 8. Pitch acceleration control system.

$$\frac{a_z(s)}{a_{zd}(s)} = \frac{(T_p\, s+1)\left(n_{p2}\, s^2 + n_{p1}\, s + 1\right)}{a_{p3}\, s^3 + a_{p2}\, s^2 + a_{p1}\, s + 1}, \tag{41}$$

where K_p, T_p, and K_q stand for the proportional, integral, and pitch damping gains, respectively. The following definitions are introduced: $n_{p1} = n_{z1}/n_{z0}$, $n_{p2} = n_{z2}/n_{z0}$, $a_{p1} = \left[T_p\left(d_{p0} + K_q\, n_{q0} + K_p n_{z0}\right) + K_p n_{z1}\right] / \left(K_p n_{z0}\right)$, $a_{p2} = \left[T_p\left(d_{p1} + K_q n_{q1} + K_p n_{z1}\right) + K_p n_{z2}\right] / \left(K_p n_{z0}\right)$, $a_{p3} = T_p\left(1 + K_p n_{z2}\right) / \left(K_p n_{z0}\right)$; $n_{z0} = Z_\alpha M_\delta - Z_\delta M_\alpha$, $n_{z1} = Z_q M_\delta - Z_\delta M_q$, $n_{z2} = Z_\delta$, $n_{q0} = \left(Z_\delta M_\alpha - Z_\alpha M_\delta\right)/u$, $n_{q1} = M_\delta$; $Z_\alpha = c_F C_{z_\alpha}$, $Z_\delta = c_F C_{z_\delta}$, $Z_q = \left(c_F d_M C_{z_q}\right) / \left(2v_M\right)$, $M_\alpha = c_M C_{m_\alpha}$, $M_\delta = c_M C_{m_\delta}$, and $M_q = \left(c_M d_M C_{m_q}\right) / \left(2v_M\right)$ for $c_F = q_\infty S_M / m$ and $c_M = q_\infty S_M d_M / I_t$.

The characteristic polynomial of the transfer function in Eq. (41) is

$$D_p(s) = a_{p3}\, s^3 + a_{p2}\, s^2 + a_{p1}\, s + 1 \tag{42}$$

K_p, T_p, and K_q can be calculated using the third-order Butterworth polynomial in Eq. (43) by placing the three poles of the control system at the desired locations specified by the desired bandwidth value (ω_c), with a damping ratio of 0.707 [4]:

$$B_3(s) = \left(1/\omega_c^3\right)\, s^3 + \left(2/\omega_c^2\right)\, s^2 + \left(2/\omega_c\right)\, s + 1 \tag{43}$$

Defining $\sigma_p = T_p/K_p$ and $\eta_p = T_p\, K_q/K_p$, σ_p, η_p, and T_p can be found by matching Eqs. (42) and (43) term by term as follows:

$$\bar{r}_p = \hat{M}_p^{-1}\, \bar{b}_p, \tag{44}$$

where $\bar{r}_p = \left[\begin{array}{ccc} \sigma_p & \eta_p & T_p \end{array}\right]^T$, $\hat{M}_p = \left[\begin{array}{ccc} 1 & 0 & n_{z2} \\ d_{p1} & n_{q1} & n_{z1} \\ d_{p0} & n_{q0} & n_{z0} \end{array}\right]$, and $\bar{b}_p = \left[\begin{array}{c} n_{z0}/\omega_c^3 \\ \left(2\, n_{z0}/\omega_c^2\right) - n_{z2} \\ \left(2\, n_{z0}/\omega_c\right) - n_{z1} \end{array}\right]$.

Regarding the rotational symmetry of the missile, as K_y, T_y, and K_r show the proportional, integral, and yaw damping gains, and n_{y1}, n_{y2}, a_{y1}, a_{y2}, and a_{y3} as well as K_y, T_y, and K_r are functions of the geometrical, dynamic, and aerodynamic parameters of the missile, the yaw plane transfer function between the desired and actual accelerations in the (a_{yd} and a_y) can be obtained as follows for $a_{zd} = a_p^c$ and $a_{yd} = a_y^c$ [4,15]:

$$\frac{a_y(s)}{a_{yd}(s)} = \frac{(T_y\, s+1)\left(n_{y2}\, s^2 + n_{y1}\, s + 1\right)}{a_{y3}\, s^3 + a_{y2}\, s^2 + a_{y1}\, s + 1} \tag{45}$$

5.2. Angle control system

A state feedback-type angle control system is introduced for the guidance commands generated by the BPG and LHG laws, by accounting the integral of the error between the reference and actual, or measured, values of the controlled state variable, i.e. flight path angle (x_i). In this scheme, the guidance commands of the BPG law about the orientation angles of the missile with respect to the ground are converted into flight path angles, as given below. LHG law commands to the flight path angles are directly utilized in the same angle control system:

$$\gamma_m^c = \theta^c - \alpha \tag{46}$$

$$\eta_m^c = \psi^c + [\beta / \cos(\theta)] \tag{47}$$

Taking gravity as an external disturbance, the next state feedback control law can be designated in the pitch plane to control γ_m:

$$u = \delta_e = k_\gamma \left(\gamma_{md} - \gamma_m\right) - k_\theta\, \theta - k_q\, q + k_i\, x_i, \tag{48}$$

where γ_{md} stands for the desired value of the flight path angle of the missile in the pitch plane. k_γ, k_θ, k_q, and k_i are the controller gains for the corresponding state variables, i.e. γ_m, θ, q, and x_i.

Expressing the equations of motion in state-space form with γ_m, θ, q, and x_i, the closed loop transfer function between the desired and actual flight path angles in the pitch plane (γ_{md} and γ_m) can be found as per the block diagram in Figure 9 [4]:

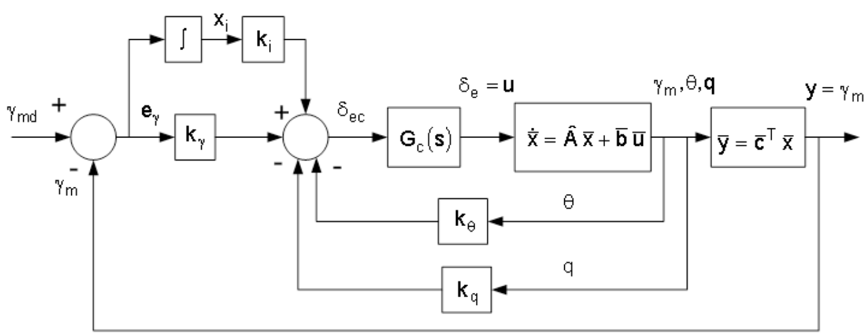

Figure 9. Flight path angle control system.

$$\frac{\gamma_m(s)}{\gamma_{md}(s)} = \frac{n_{\gamma 3}\, s^3 + n_{\gamma 2}\, s^2 + n_{\gamma 1}\, s + 1}{d_{\gamma 4}\, s^4 + d_{\gamma 3}\, s^3 + d_{\gamma 2}\, s^2 + d_{\gamma 1}\, s + 1}\,, \tag{49}$$

where $n_{\gamma 1} = (k_\gamma\, a_{\alpha\delta} + k_i\, a_{\delta q}) / (k_i\, a_{\alpha\delta})$, $n_{\gamma 2} = (a_{\alpha\delta}\, a_{\delta q}\, k_\gamma + a_{\alpha\delta}\, k_i\, Z_\delta) / (a_{\alpha\delta}\, a_{\alpha\delta}\, k_i)$, $n_{\gamma 3} = (Z_\delta\, k_\gamma) / (a_{\alpha\delta}\, k_i)$, $d_{\gamma 1} = [a_{\alpha\delta}\, (k_\theta + k_\gamma) + k_i\, a_{\delta q}] / (k_i\, a_{\alpha\delta})$, $d_{\gamma 2} = (M_\alpha + M_\delta\, k_\theta - a_{\alpha q} + a_{\alpha\delta}\, k_q + a_{\delta q}\, k_\gamma + Z_\delta\, k_i) / (k_i\, a_{\alpha\delta})$, $d_{\gamma 3} = [M_\delta\, k_q + Z_\delta\, k_\gamma - (M_q + Z_\alpha)] / (k_i\, a_{\alpha\delta})$, $d_{\gamma 4} = 1 / (k_i\, a_{\alpha\delta})$; $a_{\alpha\delta} = M_\delta\, Z_\alpha - M_\alpha\, Z_\delta$, $a_{\delta q} = M_\delta\, Z_q - M_q\, Z_\delta$, and $a_{\alpha q} = M_q\, Z_\alpha - M_\alpha\, Z_q$.

The characteristic polynomial of the transfer function in Eq. (49) becomes

$$D(s) = d_{\gamma 4}\, s^4 + d_{\gamma 3}\, s^3 + d_{\gamma 2}\, s^2 + d_{\gamma 1}\, s + 1 \tag{50}$$

The controller gains k_γ, k_θ, k_q, and k_i can be computed using the pole placement approach by regarding the forthcoming fourth-order Butterworth polynomial [4]:

$$B_4(s) = \left(1/\omega_c^4\right) s^4 + \left(2.613/\omega_c^3\right) s^3 + \left(3.414/\omega_c^2\right) s^2 + \left(2.613/\omega_c\right) s + 1 \tag{51}$$

From Eqs. (50) and (51), the matrix equation for k_γ, k_θ, k_q, and k_i appears as

$$\begin{bmatrix} k_\gamma & k_\theta & k_q & k_i \end{bmatrix}^T = \hat{M}_k^{-1}\,\bar{b}_k, \tag{52}$$

where $\hat{M}_k = \begin{bmatrix} 0 & 0 & 0 & a_{\alpha\delta} \\ Z_\delta & 0 & M_\delta & \frac{-2.613\,a_{\alpha\delta}}{\omega_c^3} \\ a_{\delta q} & M_\delta & a_{\alpha\delta} & Z_\delta - \frac{3.414\,a_{\alpha\delta}}{\omega_c^2} \\ a_{\alpha\delta} & a_{\alpha\delta} & 0 & a_{\alpha q} - \frac{2.613\,a_{\alpha\delta}}{\omega_c} \end{bmatrix}$ and $\bar{b}_k = \begin{bmatrix} \omega_c^4 \\ M_q + Z_\alpha \\ a_{\alpha q} - M_\alpha \\ 0 \end{bmatrix}$.

Similarly, the transfer function in the yaw plane can be adapted from the pitch plane transfer function by defining $n_{\eta 1}$, $n_{\eta 2}$, $n_{\eta 3}$, $d_{\eta 1}$, $d_{\eta 2}$, $d_{\eta 3}$, and $d_{\eta 4}$ [4]:

$$\frac{\eta_m(s)}{\eta_{md}(s)} = \frac{n_{\eta 3}\,s^3 + n_{\eta 2}\,s^2 + n_{\eta 1}\,s + 1}{d_{\eta 4}\,s^4 + d_{\eta 3}\,s^3 + d_{\eta 2}\,s^2 + d_{\eta 1}\,s + 1} \tag{53}$$

In this study, the angle autopilots are run in two modes. In the first mode, the bandwidth is kept at a certain value during the simulations, whereas the initial bandwidth value attains its specified final value at the end of the prescribed duration. It then remains at that value until the termination of the corresponding simulation in the second mode, where it is intended to diminish the high initial acceleration requirement of the angle-based guidance laws [4].

6. Target kinematics

To handle guidance problems against maneuvering targets, several methods, such as designing high-gain observes, are considered to estimate the target motion [16–18].

The kinematic variables of the considered ground vehicle, i.e. target, include normal and tangential acceleration components (a_T^n and a_T^t), target speed (v_T), and horizontal heading angle (η_t) with the initial values of the target velocity and heading angle (v_{T0} and η_{t0}). Integration variable σ is introduced as follows:

$$v_T(t) = v_{T0} + \int_{t_0}^{t} a_T^t(\sigma)\, d\sigma \tag{54}$$

$$\eta_t(t) = \eta_{t0} + \int_{t_0}^{t} \left[a_T^n(\sigma)/v_T(\sigma)\right] d\sigma \tag{55}$$

The time-dependent horizontal position components of the target can be modeled with the initial values x_{T0}, y_{T0}, and z_{T0} as follows:

$$x_T(t) = x_{T0} + \int_{t_0}^{t} v_T(\sigma)\, \cos\left(\eta_t(\sigma)\right) d\sigma \tag{56}$$

$$y_T(t) = y_{T0} + \int_{t_0}^{t} v_T(\sigma)\ \sin(\eta_t(\sigma))\ d\sigma \tag{57}$$

$$z_T(t) = z_{T0} \tag{58}$$

7. Missile-target engagement model

In the engagement geometry, $r_{T/M}$ represents the magnitude of $\vec{r}_{T/M}$, λ_p, and λ_y, and can be determined from the following equations:

$$r_{T/M} = \sqrt{\Delta x^2 + \Delta y^2 + \Delta z^2} \tag{59}$$

$$\lambda_p = \arctan\left[-\Delta z\ \cos(\lambda_y)/\Delta x\right] \tag{60}$$

$$\lambda_y = \arctan(\Delta y/\Delta x) \tag{61}$$

The total miss distance (d_{miss}) at $t = t_F$ can be computed from the next formula by treating the vertical component of $r_{T/M}$ to be zero, i.e. $\Delta z = 0$:

$$d_{miss} = \sqrt{\Delta x^2(t_F) + \Delta y^2(t_F)} \tag{62}$$

8. Computer simulations

PNG, VPG, APNG, BPG, and LHG laws are implemented for the zero initial heading error value of the missile against both stationary and maneuvering targets, along with the numerical values of the relevant parameters shown in Table 1. For the angle control systems with varying bandwith values, the initial values are selected to be 1 Hz, and the duration to attain the specified final value is 1 s. Aerodynamic coefficients are additionally computed for the M_∞ range of 0.3–2.7, δ_e and δ_r ranges of –10° to 10°, and α and β ranges of –17° to 19°. Depending on the current state of the missile, the appropriate values of the aerodynamic terms are continuously calculated using relevant look-up tables, prepared for the ranges given above. Similarly, the stability derivatives of the missile, which constitute one of the components of the aerodynamic terms as functions of M_∞, are computed using Missile Datcom for the pitch and roll motions of the missile against different M_∞ values (Table 2). Taking these data on the stability derivatives of the missile into account, the corresponding controller

Table 1. Essential parameters [1,19].

Parameter	Value	Parameter	Value
d_M	70 mm	Field of view of the strapdown seeker	±30°
S_M	3848.5 mm^2	Constant speed of the maneuvering target	90 km/h
L_M	2000 mm	Constant lateral acceleration of the maneuvering target	0.3·g
m	17.55 kg	Cant angle of the missile fins	0
I_a	0.0214 kg·m^2	Bandwidth of the missile control systems	5 Hz
I_t	5.855 kg·m^2	Bandwidth of the control actuation system	20 Hz
a_{max}	30 g (g = 9.81 m/s^2)	Angular excursion of the control fins	±20°
N_2 and N_3	3	Operating frequencies of the gyroscopes and accelerometers	110 Hz

gains are determined from the related expressions. The values generated for the pitch motion are used for the yaw motion with regard to the rotational symmetry of the missile [4]. The initial values of the missile and target kinematic parameters related to the engagement are presented in Table 3.

Table 2. Aerodynamic stability derivatives for the pitch and roll autopilots [4].

$\mathbf{M}_\infty$	C_{z_α}	C_{z_δ}	C_{z_q}	C_{m_α}	C_{m_δ}	C_{m_q}	C_{l_δ}
0.3	–14.966	–2.679	–33.207	0.393	20.199	–1451.030	1.358
0.5	–19.466	–4.769	–22.383	–7.407	41.794	–2240.710	0.776
1.0	–30.716	–9.993	4.676	–26.907	95.781	–4214.910	–0.680
1.5	–16.322	–3.532	–78.972	–13.094	30.080	–2526.520	0.613
2.0	–1.928	2.929	–162.620	0.719	–35.621	–838.130	1.906
2.5	12.466	9.390	–246.268	14.532	–101.322	850.260	3.199
2.7	18.224	11.974	–279.727	20.057	–127.602	1525.616	3.716

Table 3. Initial conditions of the missile and target kinematic parameters.

Parameter	Value	Parameter	Value	Parameter	Value
x_{M0}	0	p_0	50 rpm	y_{T0}	650 m
y_{M0}	450 m	q_0	5 rpm	z_{T0}	0
z_{M0}	200 m	r_0	5 rpm	v_{T0}	25 m/s (=90 km/h)
v_{M0}	408 m/s ($M_\infty = 1.2$)	α_0. β_0	0	η_{t0}	0
η_{m0}. γ_{m0}	0	x_{T0}	1000 m	a_T^t	0

The computer simulations are performed in MATLAB Simulink as per the flow chart submitted in Figure 10 for the situations given above. Their results are presented in Tables 4 and 5. The trajectories of the missile and target within the engagement scenarios for all guidance laws are given in Figures 11–15.

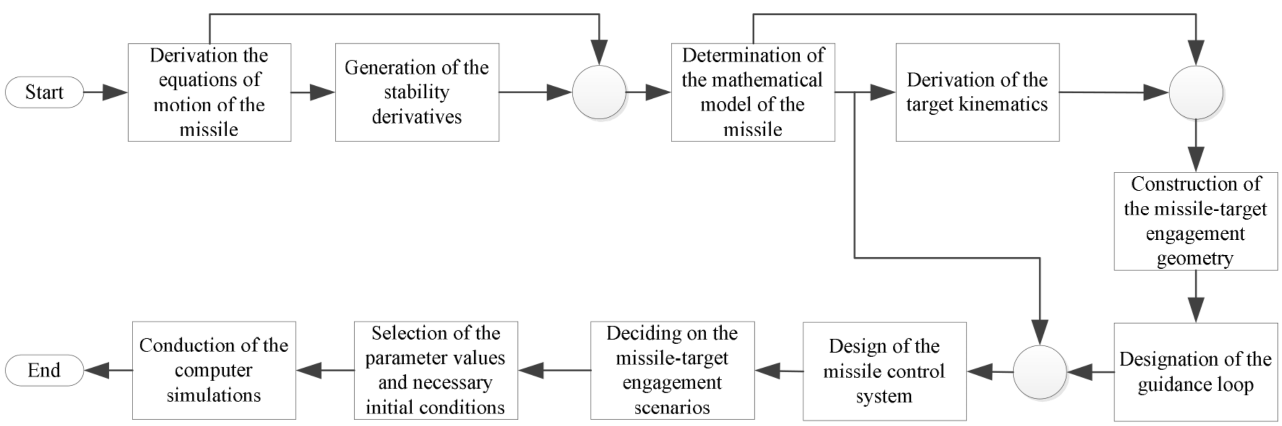

Figure 10. Flow chart for the computer simulations.

9. Discussion and conclusion

As shown in Table 4 for the constant bandwidth case, LHG law yields the smallest terminal miss distance, whereas the VPG yielding the minimum total engagement time appears to be the poorest. In fact, all total engagement values are very similar. The PNG and APNG laws demand the smallest maximum acceleration. Fortunately, the high acceleration levels of the BPG and LHG laws can be significantly reduced to the levels

Table 4. Simulation results obtained for the control systems with constant bandwidth.

Target type	Guidance law	Terminal miss distance (m)	Total engagement time (s)	Maximum acceleration requirement (g)
Stationary	PNG	3.079	2.823	3.377
	VPG	37.670	2.723	24.659
	APNG	3.079	2.823	3.377
	BPG	31.332	2.763	84.386
	LHG	1.129	2.828	32.488
Maneuvering	PNG	2.968	3.051	2.903
	VPG	63.448	2.857	14.764
	APNG	3.046	3.050	2.907
	BPG	59.436	2.868	32.496
	LHG	0.721	3.061	77.340

Table 5. Simulation results obtained for the control systems with varying bandwidth.

Target type	Guidance law	Terminal miss distance (m)	Total engagement time (s)	Maximum acceleration requirement (g)
Stationary	BPG	29.821	2.754	9.347
	LHG	2.041	2.862	13.161
Maneuvering	BPG	60.525	2.875	7.335
	LHG	2.445	3.142	17.515

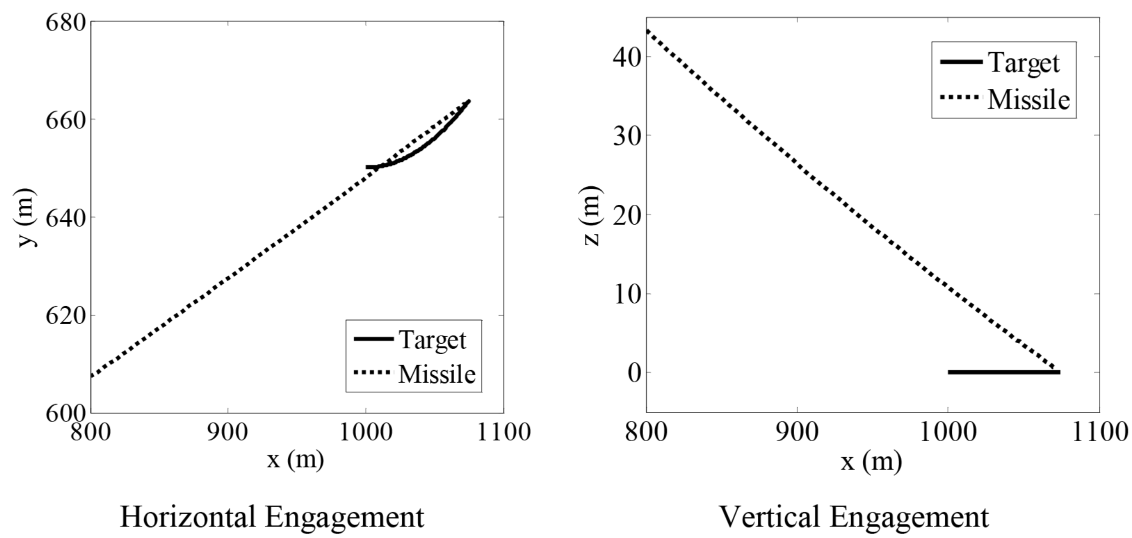

Figure 11. Engagement with the PNG law and constant-bandwidth control system.

close to the values of the acceleration-based laws, when the bandwidth of the missile control system is designated with a varying bandwidth, as tabulated in Table 5. Conversely, almost no significant changes occur in terms of terminal miss distance and total engagement in the varying bandwidth case. Moreover, no sharp trend can be seen in either increment or decrement in the data collected for the maneuvering target compared to those for the stationary target.

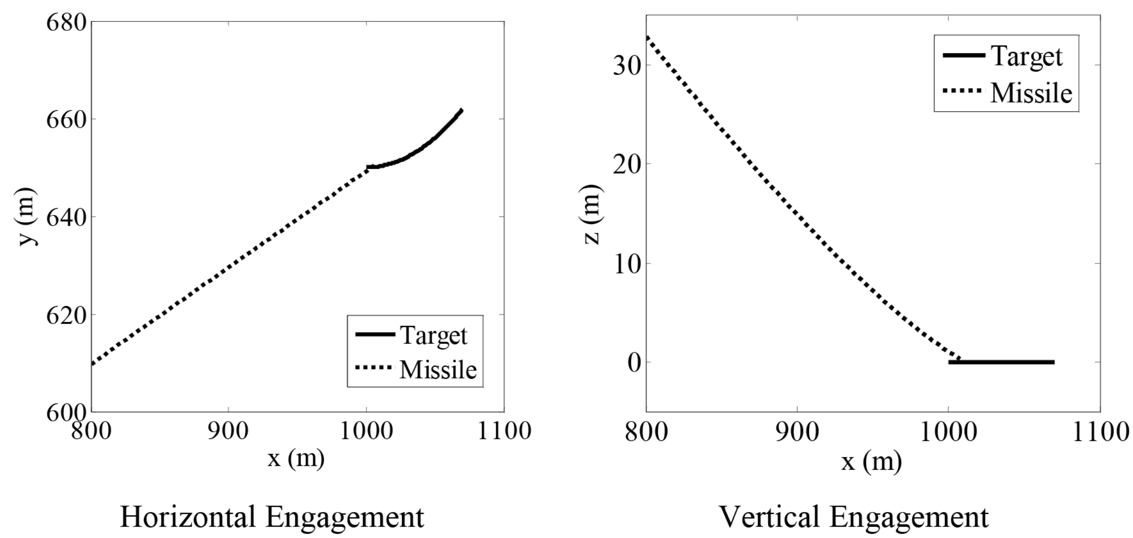

Figure 12. Engagement with the VPG law and constant-bandwidth control system.

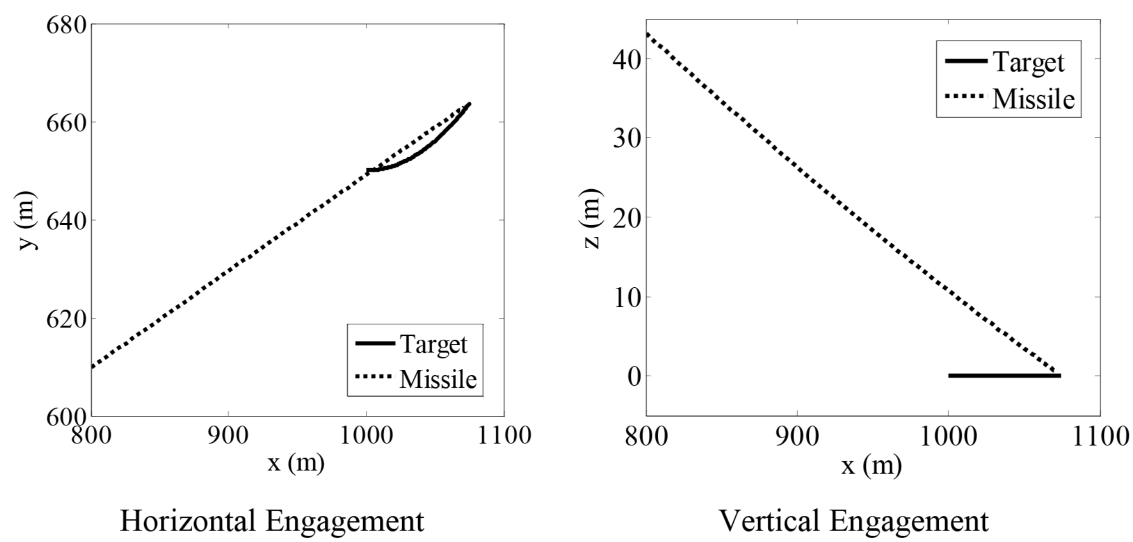

Figure 13. Engagement with the APNG law and constant-bandwidth control system.

In order to apply the proposed methods on a real missile system, convenient electronic cards should be designed, including driving and power control cards and a satisfactory control actuation system. Furthermore, corresponding sensors and electronic components with cables and connectors should be procured. Once the resulting guidance constants and controller gains are embedded into the relevant electronic cards in matrix form and have made the required fine tunings in the laboratory, they can be mounted onto the related missile body and tested again in their original casings. Unfortunately, there was no opportunity to implement the present guidance and control algorithm on a real missile. Hence, only the presented simulation results are in hand to demonstrate the usefulness of the proposed scheme. In most guided missiles, PNG law is chosen against stationary or slow-moving targets along with an acceleration control system. CİRİT air-to-surface missiles developed by ROKETSAN Inc. can be given as an example for the mentioned kind of missiles. In real missile systems, accelerometers and gyros are utilized to measure the three components of the relative linear

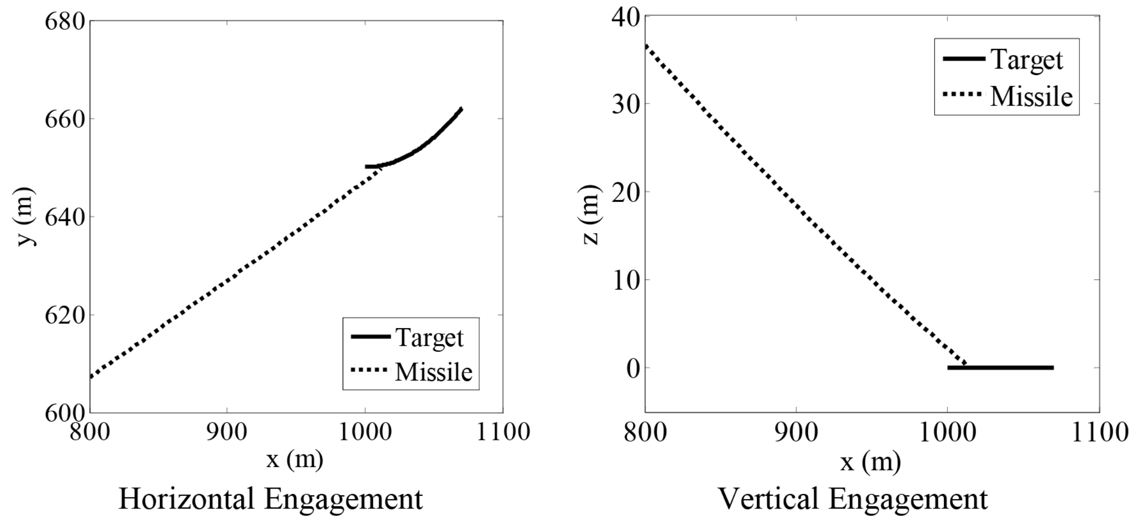

Figure 14. Engagement with the BPG law and constant-bandwidth control system.

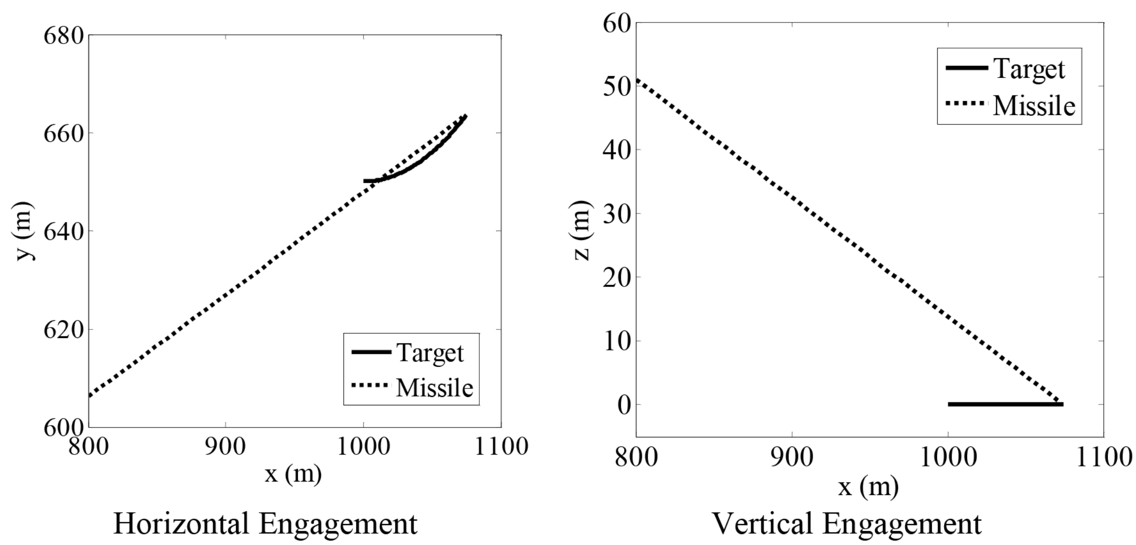

Figure 15. Engagement with the LHG law and constant-bandwidth control system.

accelerations and angular speeds of the missile, respectively. Resolvers, incremental or absolute type encoders, or potentiometers are used as feedback elements for the control actuation systems to acquire the angular position information as per the accuracy requirements.

It can be concluded that none of the acceleration- and angle-based guidance laws is absolutely superior. Therefore, a convenient guidance law should be selected depending on the engagement conditions.

References

[1] Zarchan P. Tactical and Strategic Missile Guidance. 1st ed. Washington, DC, USA: AIAA, 1994.

[2] Zarchan P. Ballistic missile defense guidance and control issues. Sci Gl Sec 1998; 8: 99-124.

[3] Yang CD, Hsiao FB, Yeh FB. Generalized guidance law for homing missiles. IEEE T Aerosp Electron Syst 1989: 25: 197-212.

[4] Özkan B. Dynamic modeling, guidance, and control of homing missiles. PhD, Middle East Technical University, Ankara, Turkey, 2005.

[5] Özkan B, ÖzgÖren MK, Mahmutyazıcıoğlu C. Investigation of the performance of the single- and two-part missiles against moving surface targets In: 2007 National Meeting of Automatic Control; 1315 June 2007; Sabancı University, İstanbul, Turkey. (article in Turkish with an abstract in English).

[6] Lin CF. Modern Navigation, Guidance and Control Processing. Upper Saddle River, NJ, USA: Prentice Hall, 1991.

[7] Özkan B, ÖzgÖren MK, Mahmutyazıcıoğlu G. Notable guidance methods that can be applied to homing missiles. In: 2008 Defence Technologies Congress; 2731 July 2008; Ankara, Turkey (article in Turkish with an abstract in English).

[8] Blakelock JH. Automatic Control of Aircraft and Missiles. 1st ed. Somerset, NJ, USA: Wiley, 1965.

[9] Özkan B, ÖzgÖren MK, Mahmutyazıcıoğlu G. Guidance and control of two-part homing missiles using the proportional navigation guidance law. In: AIAA 2008 Guidance, Navigation, and Control Conference and Exhibit; 1821 August 2008; Honolulu, HI, USA. Reston, VA, USA: AIAA.

[10] Şahin KD. A pursuit evasion game between an aircraft and a missile. MSc, Middle East Technical University, Ankara, Turkey, 2002.

[11] Berglund E. Guidance and control technology. In: RTO SCI 2000 Lecture Series on Technologies for Future Precision Strike Missile Systems; 2324 March 2000; Atlanta, GA, USA. pp. 1-10.

[12] ÖzgÖren MK. Some remarks on rotation sequences and associated angular velocities. J Mech Mach Theory 1994; 29: 933-940.

[13] Budiyoo A, Rachman H. Proportional guidance and CDM control synthesis for a short-range homing surface-to-air missile. J Aerosp Eng 2012; 25: 168-177.

[14] Özkan B, ÖzgÖren MK, Mahmutyazıcıoğlu G. Implementation of linear homing guidance law on a two-part homing missile. In: IFAC 2008 World Congress; 611 July 2008; Seoul, Korea. New York, NY, USA: IFAC. pp. 13999-14004.

[15] Özkan B, ÖzgÖren MK, Mahmutyazıcıoğlu G. Comparison of the acceleration- and angle-based guidance laws for a short-range air-to-surface missile. IFAC Proc 2011; 44: 3527-3532.

[16] Ma K, Khalil HK, Yao Y. Guidance law implementation with performance recovery using an extended high-gain observer. Aerosp Sci Technol 2013; 24: 177-186.

[17] Li GL, Yan H, Ji HB. A guidance law with finite time convergence considering autopilot dynamics and uncertainties. Int J Control Autom Syst 2014; 12: 1011-1017.

[18] Kada B. Arbitrary-order sliding-mode-based homing-missile guidance for intercepting highly maneuverable targets. J Guid Control Dynam 2014; 37: 1999-2013.

[19] Laser Seeker System Workshop. Martin Marietta Training Notes, 1993.